AIP | Journal of Applied Physics

Electromigration induced stress evolution under alternate current and pulse current loads

V. Sukharev, X. Huang, and S. X.-D. Tan

Citation: Journal of Applied Physics **118**, 034504 (2015); doi: 10.1063/1.4926794
View online: http://dx.doi.org/10.1063/1.4926794
View Table of Contents: http://scitation.aip.org/content/aip/journal/jap/118/3?ver=pdfcov
Published by the AIP Publishing

Electromigration induced stress evolution under alternate current and pulse current loads

V. Sukharev,[1] X. Huang,[2] and S. X.-D. Tan[2]
[1]*Mentor Graphics Corporation, Fremont, California 94538, USA*
[2]*University of California, Riverside, California 92521, USA*

(Received 18 March 2015; accepted 3 July 2015; published online 15 July 2015)

Stress evolution in a metal line embedded in a rigid confinement caused by the arbitrary wave-form time-dependent current loads is resolved by a direct analytic solution of the one-dimensional (1-D) Korhonen's equation. Electromigration induced stress buildup and relaxation kinetics resulted by time-dependent current density are obtained as functions of the relevant physical parameters. A novel methodology for physics based conversion between the time-dependent and effective DC current densities is developed based on a condition of equal void nucleation times resulted by these currents. It is shown that in the case of high frequency currents, with periods much smaller than the characteristic time of stress evolution, the stress buildup is proportional to the pulse duty factor. It is demonstrated that very short metal lines with preexisted thermal voids loaded with symmetrical bi-directional currents can demonstrate a notable resistance increase when a specific temperature oscillation is generated in the line by active devices of the integrated circuit. © *2015 AIP Publishing LLC*. [http://dx.doi.org/10.1063/1.4926794]

I. INTRODUCTION

Electromigration (EM) induced degradation of the electrical resistance of test structures is traditionally monitored by applying the DC stressing. A majority of proposed physical models describing the EM phenomenon is also assumed the DC load. At the same time, all semiconductor integrated circuit (IC) chips operate with time-dependent, for example, pulse electric current. Everyday practice demonstrates that the EM-induced failures continue to be the primary killer of the on-chip interconnects. Well known EM-induced voiding is responsible for the interconnect line resistance increase, while the hillock formation can generate the electrical short induced failure. This paper concentrates on the void-induced electric circuit degradation due to its more frequent appearance. There are two major functions of the on-chip interconnect, namely, are providing a connectivity between different parts of a design for proper signal propagating, and delivering a needed amount of voltage to each cell. While the resistance degradation of the individual segments of interconnect circuits can destroy both these functions, the role of EM is quite different in degrading the power supply chain and the signal circuits. The difference is in the types of electric currents employed in these two cases. Indeed, the majority of signal lines carry bidirectional pulse currents and, hence, are characterized by very long times to the EM-induced failure. It is caused by a repetitive increase and decrease of the mechanical stress at the segment ends, caused by atom accumulations and depletions due to a momentum exchange with the conduction electrons. In contrast, power lines carrying unidirectional pulse currents can fail in much shorter times due to continues stress buildup under EM action. Thus, we can conclude that in the majority of cases, the EM induced chip failure is happening when interconnect cannot deliver needed voltage to any gate of the circuitry.[1] Since the time-dependent nature of the current density, the different conversion factors have been introduced to predict an electric degradation of the on-chip interconnects caused by transient currents on the basis of well understood DC current induced degradation. These factors are used by chip designers for designing the EM resilient chips and for the final design sign-off verification.

A number of physics based models have been developed to describe the EM phenomenon under the time-dependent current stressing.[2–6] Majority of the models describe an evolution of the vacancy concentration in a metal line confined by the rigid dielectric caused by AC/pulse currents. EM-induced evolution of the mechanical stress, which, based on a general consensus, is a main cause of the void growth resulting the resistance degradation, was not properly considered. The first part of the paper describes the stress evolution in the initially void-less metal line loaded with the time-dependent electric current. It is obtained by a direct solution of the 1-D continuity equation. Derived analytic solutions describe an ability of different waveforms of electric loads to develop a stress exceeding the critical one, which is required for creating a condition for a stable growth of the preexisted micro-flaws. Particularly, the derived formalism predicts immortality of the lines loaded with symmetric bidirectional currents. But, the experiments demonstrate that in some cases, the lines fail under an action of AC and symmetrical bidirectional pulse currents. In addition to the described in literature, a void-induced failure caused by the thermal fatigue,[13] which is generated even in the absence of any current, the second part of the paper proposes another possible mechanism of failure caused by symmetrical bidirectional currents. Very short metal lines with preexisted thermal voids, which are loaded with such bidirectional currents, can demonstrate a notable resistance increase when a specific temperature oscillation takes place at the line location.

II. STRESS EVOLUTION IN CONFINED METAL LINES: 1-D PHENOMENOLOGICAL THEORY OF ELECTROMIGRATION

A. Pre-voiding kinetics of stress evolution under DC current load

In a simple 1-D approximation, which was used by Korhonen,[7] for deriving a model of the stress evolution in a confined and electrically loaded metal line, a standard assumption was employed: the divergence of the atomic flux Γ_A generates a volumetric strain θ

$$\frac{\partial\theta}{\partial t} = \Omega\frac{\partial\Gamma_A}{\partial x}. \tag{1}$$

Here, Γ_A is a total atomic flux comprised by the fluxes caused by the EM force and stress gradient

$$\Gamma_A = \frac{D_a}{\Omega k_B T}\left[eZ * \rho j + \frac{\partial\sigma_{Hyd}}{\partial x}\right]. \tag{2}$$

Here, D_a is the effective atomic diffusivity, eZ is the effective charge of migrating atoms, B is the effective bulk elasticity modulus, Ω is the atomic lattice volume, ρ is the metal resistivity, j is the current density, k_B is the Boltzmann constant, T is the temperature, x is the coordinate along the line, and t is time. We assume here that the lattice atom concentration is taken as $N_a = 1/\Omega$. Substituting the total flux Γ_A and the volumetric strain as $\theta = \sigma_{Hyd}/B$ in (1) provides

$$\frac{\partial\sigma_{Hyd}}{\partial t} = \frac{\partial}{\partial x}\frac{D_a B\Omega}{k_B T}\left(\frac{eZ\rho j}{\Omega} + \frac{\partial\sigma_{Hyd}}{\partial x}\right). \tag{3}$$

Equation (3) is the well-known Korhonen's equation describing evolution of the stress distribution along the confined metal line caused by the applied electric current.[7] A number of the simplifying assumptions are adopted: it is assumed that the atom diffusivity does not depend on stress; vacancy concentration is in the equilibrium with stress at any instant in time everywhere including grain interior; stress evolution is caused just by the atomic flux divergence, the additional stress evolution due to vacancy equilibration with the stress is not accounted. It should be mentioned, while the derivation of Eq. (3) was done for 1-D line, the employed effective valence Z and atomic diffusivity D_a allow accounting some elements of wire texture and 3-D geometry.[8]

A solution to this initial-boundary value problem in the case of a finite line with the diffusion blocking ends located at $x = 0$ and L, where L is the line length, loaded with the DC current j was obtained by the method of separation of variables in Ref. 7

$$\sigma_{Hyd} = \sigma_T - \frac{eZ\rho jL}{\Omega} \times\left(\frac{x}{L} - \frac{1}{2} + 4\sum_{n=0}^{\infty}\frac{\cos\left(\frac{(2n+1)\pi x}{l}\right)}{(2n+1)^2\pi^2}e^{-\kappa\frac{(2n+1)^2\pi^2}{L^2}t}\right). \tag{4}$$

Here, σ_T is the residual stress preexisting in the line, $\kappa = D_a B\Omega/k_B T$, and $D_a = D_0\exp(-E_a/k_B T)$. Figure 1 shows the evolution of the hydrostatic stress distributed along the line, in the case of zero initial stress. At long times, this solution provides the result, originally obtained by Blech and Herring,[9]: $\sigma_{Hyd}(x, t=\infty) = \sigma_T - eZ\rho j\left(x - \frac{L}{2}\right)/\Omega$. It was agreed that development of the so-called critical stress σ_{Crit} should be used as a condition for a stable growth of the preexisted flows. Indeed, due to huge activation energy a void cannot be nucleated by a vacancy agglomeration even when the stress is big. At the same time, different flaws such as micro cracks, small process induced cavities (pores), dislocation induced crystallographic steps, etc., can preexist in metal. The classical model of the homogeneous nucleation,[10] provides that a cavity, located in the metal loaded with the hydrostatic tensile stress σ, can either shrink or enlarge depending on the cavity size R. In a very rough approximation, which we use only for the illustrative purposes, if $R < Rc = 2\gamma/\sigma$, where γ is the surface energy per unit area, the cavity will shrink to reduce the free energy of the system representing metal with the cavity, if $R > Rc$, the cavity will enlarge to reduce this energy. Thus, assuming that the preexisting cavities are of the 5–10 nm size, we can estimate the critical stress level as of $\sigma \approx 200 - 500$ MPa when $\gamma \approx 1\,\mathrm{N/m^2}$. It means, if stress exceeds the critical level then the preexisting cavities of the corresponding sizes start to grow. Rate of this grow is determined by the atom diffusion, i.e., is pretty much slow.

B. Stress evolution caused by the time-dependent current

Solution of the continuity Eq. (3) with a time-dependent current can be obtained by converting it to the nonhomogeneous form

$$\frac{\partial\left(\sigma + \frac{eZ\rho j}{\Omega}\left(x - \frac{L}{2}\right) - \sigma_T\right)}{\partial t} - \kappa\frac{\partial^2}{\partial x^2}\left(\sigma + \frac{eZ\rho j}{\Omega}\left(x - \frac{L}{2}\right) - \sigma_T\right) = \frac{eZ\rho j}{\Omega}\left(x - \frac{L}{2}\right)\frac{\partial j}{\partial t} \tag{5}$$

with same diffusion blocking BC: $\partial\sigma/\partial t|_{x=0,l} = -eZ\rho j/\Omega$, and initial condition $\sigma(x, t=0) = \sigma_T$ that are used in Eq. (3). Introduction of new variables: $u(x,t) = \sigma + \frac{eZ\rho j}{\Omega}\left(x - \frac{L}{2}\right) - \sigma_T$, and $h(x,t) = \frac{eZ\rho j}{\Omega}\left(x - \frac{L}{2}\right)\frac{\partial j}{\partial t}$ allows us to convert the considered case with nonhomogeneous BC to the case with the homogeneous BC $\partial u/\partial t|_{x=0,l} = 0$. The latter allows to implement the standard solution procedure of the cosine series expansion for $u(x,t)$ and $h(x,t)$. Solution to Eq. (5) takes the form

$$\sigma(x,t) = \sigma_T + \frac{4eZ\rho}{\Omega L}\kappa\sum_{n=0}^{\infty}\cos\frac{(2n+1)\pi x}{L} \times e^{-\kappa\frac{(2n+1)^2\pi^2}{l^2}t}\int_0^t j(t)e^{\kappa\frac{(2n+1)^2\pi^2}{L^2}\tau}d\tau. \tag{6}$$

It is easy to show that substituting in (6), the time-dependent current density $j(t)$ with the DC current density j and using

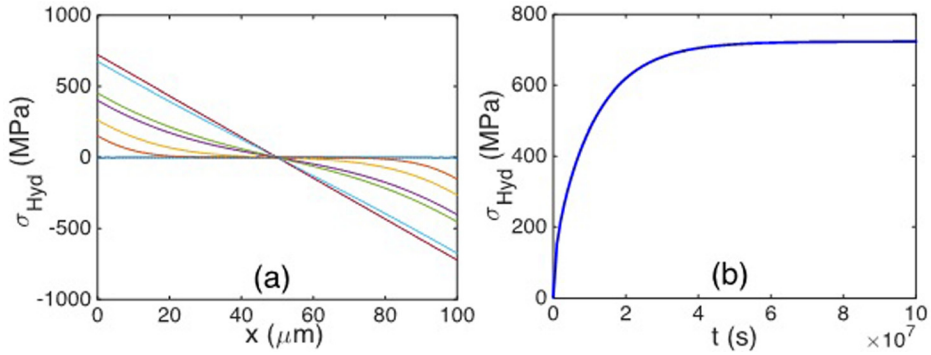

FIG. 1. Evolution of the hydrostatic stress (a) along the metal line loaded with DC current, and at the cathode end of line, (b) $j = 5 \times 10^9$ A/m^2, T = 400 K.

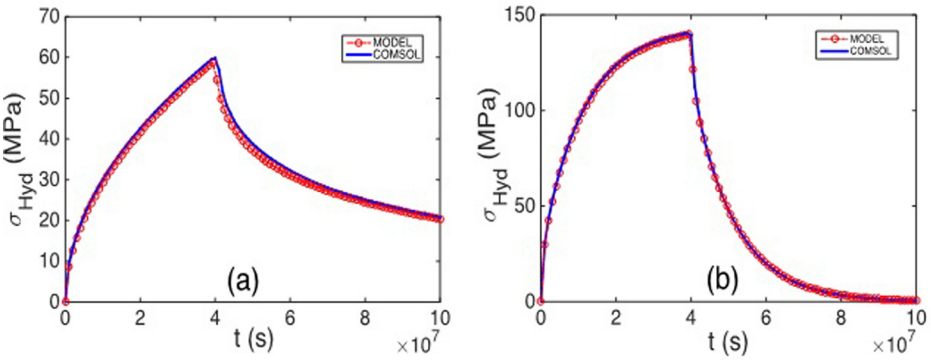

FIG. 2. Stress relaxation at T = 373 K (a) and T = 400 K (b).

the relation $4\sum_{n=0}^{\infty}\frac{\cos\left(\frac{(2n+1)\pi x}{L}\right)}{(2n+1)^2\pi^2} = \frac{1}{2} - \frac{x}{L}$ results in the classic stress evolution described by (4).

If at the instant in time t = t*, the current is switched-off then the stress will start to relax. Stress relaxation kinetics, which is obtained from the solution of Eq. (5) with the initial condition given by (6) at t = t*, has the form

$$\sigma(x, t \geq t^*) = \sigma_T + \frac{4eZ\rho}{\Omega L}\kappa\sum_{n=0}^{\infty}\cos\frac{(2n+1)\pi x}{L} \times e^{-\kappa\frac{(2n+1)^2\pi^2}{L^2}t}\int_0^{t^*} j(t)e^{\kappa\frac{(2n+1)^2\pi^2}{L^2}\tau}d\tau. \quad (7)$$

Solution (7) describes the relaxation of stress accumulated during the time interval [0, t*]. Relaxation is described by an exponential decay with the partial time constants $\tau_0^{(2n+1)} = L^2/\kappa\pi^2(2n+1)^2 = \tau_0/(2n+1)^2$, determined by the atomic diffusivity. Figure 2 shows the relaxation kinetics of stresses accumulated at the cathode end of line during 4×10^7 s of stressing by DC current with the density of 1×10^9 A/m^2 at T = 373 K and 400 K. This kinetics was calculated with the derived analytic expression (7) and by the numerical solution of Eq. (3) with the finite-element analysis (FEA) tool COMSOL.[11] All numerical calculations have been performed with following parameters $B = 1 \times 10^{11}$ Pa, $\Omega = 1.66 \times 10^{-29}$ m^3, $k_B = 1.38 \times 10^{-23}$ J/K, $L = 1 \times 10^{-4}$ m, $\sigma_T = 0$, $Z = 10$, $e = 1.6 \times 10^{-19}$ q, $\rho = 3 \times 10^{-8}$ Ohm × m, $D_0 = 7.56 \times 10^{-5}$ m^2/s, and $E_a = 1.28 \times 10^{-19}$ J.

Stress evolutions caused by unipolar (unidirectional) pulse current (UPC) with the density j_+, pulse period T, and pulse time t_+, (Figure 3), taking place at T = 373 K and T = 400 K are shown in Figure 4. The corresponding formulas describing this kinetics, which were obtained by the direct solution of Eq. (5), are shown in Appendix A. Figure 4 shows the stress evolution caused by the unipolar pulse ($t_+ = 1 \times 10^7$ s and $T = 2 \times 10^7$ s) current with the density of 1×10^9 A/m^2 at T = 373 K and 400 K. Figure 4(b) demonstrates the fast saturation of the developed stress caused by a fast stress relaxation occurring between the pulses, which happens at the elevated temperatures. Solutions to Eq. (5) for the bipolar (bidirectional) pulse currents (BPC) with the different positive and negative current densities j_+ and j_-, pulse periods T and positive and negative phase durations t_+ and t_- are shown in Fig. 5. It shows the stress evolution caused by a bipolar symmetrical pulse ($t_+ = 1 \times 10^7$ s and $t_- = 1 \times 10^7$ s) current density of 1×10^9 A/m^2 at T = 373 K. All these results were predicted by (A1)–(A4) and with COMSOL based numerical solution of Eq. (3).

All demonstrated above results have been obtained for the slow varying current densities. The positive and negative parts of the pulse have last about 100 days. These long time intervals allow the system to reach new equilibrium states corresponded the applied currents by means of metal atom diffusion. Contrary to this case, the conventional semiconductor chips operate at the MHz and GHz frequencies. Figure 6 demonstrates the stress evolution caused by the applied 1 MHz symmetrical and nonsymmetrical BPC, with

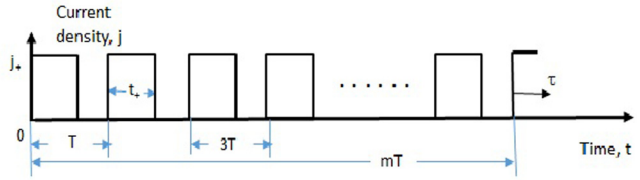

FIG. 3. Schematics for the unipolar pulse current.

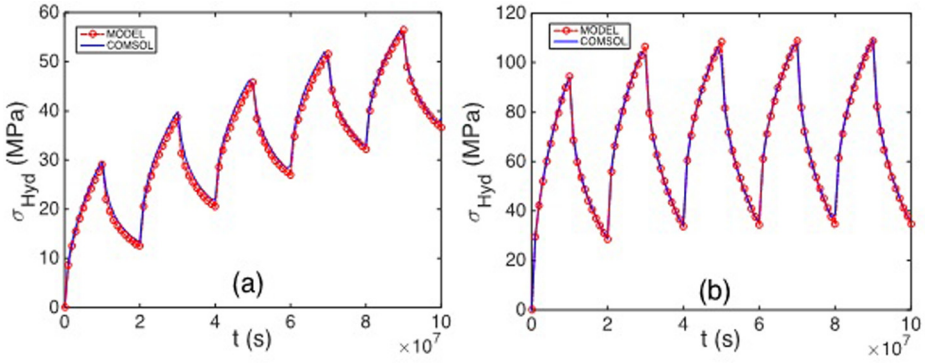

FIG. 4. Stress evolution caused by the unipolar pulse current at T = 373 K (a) and T = 400 K (b).

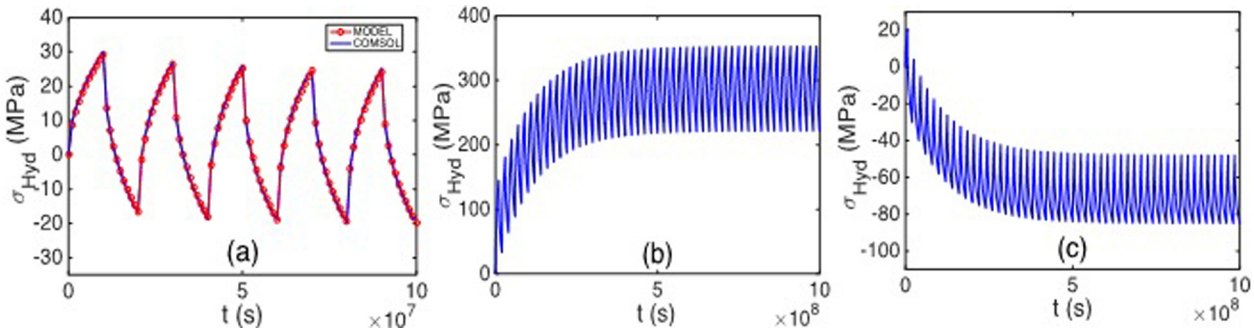

FIG. 5. Stress evolution caused by bipolar symmetrical pulse ($t_+ = 1 \times 10^7$ s and $t_- = 1 \times 10^7$ s) current density of 1×10^9 A/m^2 taking place at T = 373 K, (a); long-term stress kinetics caused by BPC with $j_+ = 5 \times 10^9$ A/m^2 and $j_- = -1 \times 10^9$ A/m^2, $t_+ = 1 \times 10^7$ s and $t_- = 1 \times 10^7$ s, (b), and with $j_+ = 1 \times 10^9$ A/m^2 and $j_- = -1 \times 10^9$ A/m^2, $t_+ = 0.5 \times 10^7$ s and $t_- = 1.5 \times 10^7$ s, (c) at T = 373 K.

the characteristic pulse time of 5×10^{-7} s. It can be seen that these stress evolutions caused by high frequency pulse currents correspond well to the stress evolutions caused by the pulse averaged DC currents $j = (j_+t_+ + j_-t_-)/T$, shown in Figure 6 by solid lines. This result can be easily derived from the BPC stress evolution kinetics (A2) and (A4). Indeed, remembering that in this case for all involved time intervals we have: T, t_+, $t_- \ll \tau_0$, we can expand all exponents in series and keep just liner terms. It provides

$$\sigma = \sigma_T - \frac{eZ\rho L}{\Omega}\left(\frac{j_+t_+ - |j_-|t_-}{T}\right) \times \left(\frac{x}{L} - \frac{1}{2} + 4\sum_{n=0}^{\infty}\frac{\cos\left(\frac{(2n+1)\pi x}{L}\right)}{(2n+1)^2\pi^2} e^{-\kappa\frac{(2n+1)^2\pi^2}{L^2}t}\right) + O\left(\frac{j_+t_+ - |j_-|t_-}{\tau_0}\right), \quad (8)$$

where $O((j_+t_+ - |j_-|t_-)/\tau_0)$ is the term providing small ($\sim$0.01 MPa) fluctuations around the curve describing the stress evolution under effective DC currents, shown in Fig. 6.

Hence, in the cases of high frequency pulse currents, which are typical for the standard cells operation in IC chips, the accumulated stress distributions along the intra-cell metal lines correspond to the stresses caused by the effective DC currents with the values scaled proportionally to the pulse duty factors: $(j_+t_+ - |j_-|t_-)/T$ - in the case of bidirectional currents, and j_+t_+/T - in the case of unidirectional pulse currents, Fig. 6. However, the lengths of the metal lines located inside cells are so short, which are of the order of micron or less that any essential stress buildup should not be expected. It means that EM cannot be responsible for the resistance degradation in the IC standard cells, caused by the stress-induced void nucleation and growth, which is discussed in literature.[12]

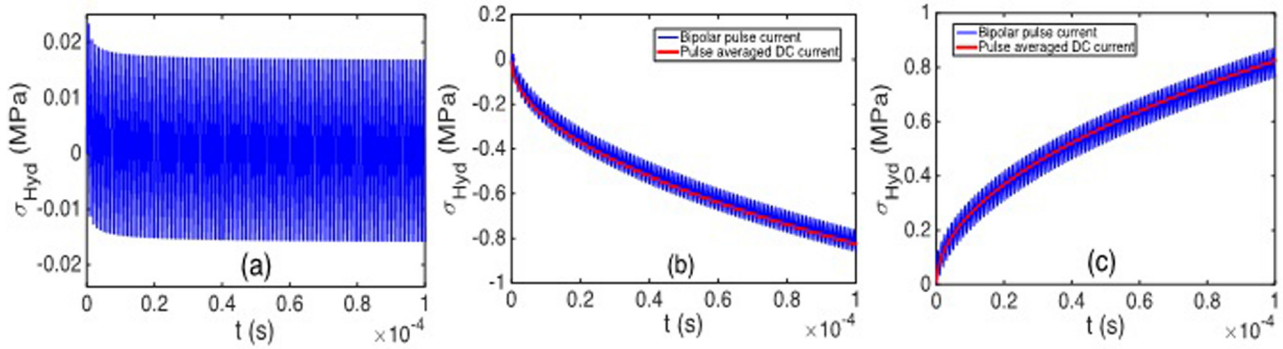

FIG. 6. Stress evolution in the metal line caused by high frequency (1 MHz) bipolar pulse currents: with $j_+ = 1 \times 10^9$ A/m^2 and $j_- = -1 \times 10^9$ A/m^2, (a), $j_+ = 1 \times 10^9$ A/m^2 and $j_- = -5 \times 10^9$ A/m^2, (b), $j_+ = 5 \times 10^9$ A/m^2 and $j_- = -1 \times 10^9$ A/m^2, (c) at T = 500 K.

Quite different situation with the time-dependent current densities exists in the power/ground nets. Small background DC currents distributed across the grid are perturbed with the unipolar pulses generated by switching cells. An intensity of these perturbations depends on the activity factors of standard cells, which are different for different workloads. In general, total current passing between the neighbor power vias is a pulse current. Unidirectional current and the long length of the power net segments can provide the conditions for σ_{Crit} accumulation. In this case, the criterion for determination of the effective DC current can be established. Since the development of the critical stress is a commonly accepted criterion for originating the failure, we employ it for the calculation of the effective DC current on the basis of known time-dependent current. Taking expressions (4) and (6) at x = 0, which means the time evolution of the stress at the cathode edge of line, and keeping just slowly decaying terms provides

$$j_{DC}^{eff} = \frac{1}{\tau_0} \frac{e^{-\frac{t_{nuc}}{\tau_0}}}{1 - e^{-\frac{t_{nuc}}{\tau_0}}} \int_0^{t_{nuc}} j(\tau) e^{\frac{\tau}{\tau_0}} d\tau. \quad (9)$$

Here, $\tau_0 = L^2/\kappa\pi^2 = k_B T L^2/D_a B\Omega\pi^2$ and t_{nuc} is the void nucleation time in the case of a time-dependent load. Assuming that the void nucleation time is much longer than τ_0, the expression (9) takes the form

$$j_{DC}^{eff} = \frac{1}{\tau_0} \int_0^{t_{nuc}} j(\tau) e^{-\frac{\tau}{\tau_0}} d\tau = \frac{D_a B\Omega\pi^2}{k_B T L^2} \int_0^{t_{nuc}} j(\tau) e^{-\frac{D_a B\Omega\pi^2}{k_B T L^2}\tau} d\tau. \quad (10)$$

Hence, the effective DC current depends on all relevant physical parameters describing the stress relaxation phenomenon. The dependence of j_{DC}^{eff} on the line length, effective atomic diffusivity as well as the bulk modulus B indicates on the important role played by the line geometry and the metal texture. Small grains and fast diffusivities on the GB and interfaces make the effective DC current larger. Conversion formula (10) is valid when the void nucleation step is a limiting step for the failure development, which is, for instance, 10% increase in the line resistance. In the case when the void growth, which is responsible for the resistance change, is a limiting step, the effective DC current density should be determined from the condition of the equal times required for developing $\Delta R = 0.1 \times R_0$ by each, the time-dependent and effective DC currents.

III. RESISTANCE DEGRADATION IN THE SHORT METAL LINES CAUSED BY THE SYMMETRICAL BIDIRECTIONAL CURRENT

Results, that were obtained above, indicate that even long metal lines loaded with the symmetrical bipolar pulse or AC currents will never failed since the EM-induced accumulation of the critical stress required for voiding or hillock formation is never happened. Nevertheless there are a good number of papers providing the experimental proof of failures generated by this type of stressing.[3,4,14–16] One of the possible answers for this paradox can be found in the paper of Moning *et al.*,[13] where the identical defects were found in all three lines located in a close proximity to each other in the test structure with two outer lines loaded with the sinusoidal voltages and the middle line was not carrying any current. The temperature oscillations generated by the outer lines have resulted in the identical defects in all three lines. Authors have concluded that the thermal fatigue controlled by diffusive mechanism and interface properties was responsible for these defects. A difference between these fatigue-based defects and the EM-induced voids is a mobility of the later under the action of electric current, which can be observed, for example, by SEM studies.[17]

Another possible mechanism of failure caused by symmetrical bidirectional currents is the growth of a void, which was formed in the line as the result of thermal stress relaxation.[8] Very short metal lines with preexisted thermal voids, loaded with such bidirectional currents, can demonstrate a notable resistance increase when a specific temperature oscillation is generated. In order to prove the existence of this mechanism, we need to develop a formalism describing an evolution of the metal line resistance caused by the current induced evolution of the void volume. As it was discussed,[8] a metal line embedded in the rigid confinement and cooled from the zero stress temperature down to the test temperature can reach two different states of equilibrium. One of them is the state with a uniformly distributed tensile stress, which was generated in the line due to a difference in the coefficients of thermal expansion (CTE) of the metal and surrounding. Another one is characterized by the presence of a void, which volume is determined by the relaxation of the preexisted tensile strain, and by zero stress everywhere else in the metal. It should be mentioned that generated thermal stress should exceed the critical stress, which is required for void nucleation. The later state is the only stable equilibrium state for the metal line with the large tensile stress.[8] When an electrical stressing is applied to this line, a void, if it is located at the line end, starts changing its volume. In the case of DC stressing, a void located at the cathode end of line will be growing by means of migration of the void surface atoms to the metal bulk. A corresponding kinetics of the evolution of stress distribution along the line was obtained from the solution of Eq. (3), with the zero stress and zero flux BC at the void edge and the anode end of line, correspondingly, in Refs. 18 and 19

$$\sigma(x,t) = -\frac{eZ\rho jL}{\Omega}\left[\frac{x}{L} - \frac{8}{\pi^2}\sum_{k=0}^{\infty}(-1)^k \frac{\sin\frac{(2k+1)\pi x}{2L}}{(2k+1)^2} e^{-\kappa\frac{(2k+1)^2\pi^2}{4L^2}t}\right]. \quad (11)$$

Void volume evolution, calculated as $V(t) = -\int_0^L \frac{\sigma(x,t)}{B} dx$, has the form

$$V(t) = V_{sat}\left[1 - \frac{32}{\pi^3}\sum_{k=0}^{\infty}\frac{(-1)^k}{(2k+1)^3} e^{-\kappa\frac{(2k+1)^2\pi^2}{4L^2}t}\right]. \quad (12)$$

Here, $V_{sat} = WH\frac{eZ\rho jL^2}{2\Omega B}$ is the void saturation volume, which is developed when the EM-induced atomic flux is balanced by the stress gradient induced flux,[8] W, H, and L are the line

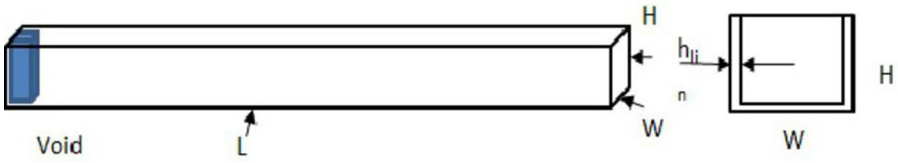

FIG. 7. Schematics of the line geometry.

width, thickness, and length schematically shown in Fig. 7. Assuming that the growing void expands through the line cross-section, and that Ta/TaN liner conducts the electric current in the portion of line occupied by the void, the change of the line resistance caused by the growing void can be presented as

$$\Delta R(t) = \frac{V(t)}{WH}\left(\frac{\rho_{TaN}}{h_{lin}(W+2H)} - \frac{\rho_{Cu}}{WH}\right), \tag{13}$$

where h_{lin} is the liner thickness, and ρ_{TaN} and ρ_{Cu} are the resistivity of the liner and the line bulk metal (copper). Thus, in the case of DC stressing with the current density j, the kinetics of line resistance change is described as

$$\Delta R(t) = \frac{eZ\rho jL^2}{2\Omega B}\left(\frac{\rho_{TaN}}{h_{lin}(W+2H)} - \frac{\rho_{Cu}}{WH}\right) \times \left[1 - \frac{32}{\pi^3}\sum_{k=0}^{\infty}\frac{(-1)^k}{(2k+1)^3}e^{-\kappa\frac{(2k+1)^2\pi^2}{4L^2}t}\right]. \tag{14}$$

Fig. 8 shows this kinetics caused by two different current densities of 3×10^9 A/m^2 and 5×10^9 A/m^2. It can be seen that if the resistance change caused by the saturated void does not exceed the critical, which is taken as 10% of R_0 ($\Delta R_{crit} = 0.1 \times R_0$) in the example shown in Fig. 8, the line is immortal. All calculations are done with the same physical parameters that were used in Section II and with the following line geometries: $L = 1\,e^{-6}$ m; $h_{lin} = 10\,e^{-9}$ m; $H = 120\,e^{-9}$ m; $W = 200\,e^{-9}$ m; and the liner resistivity $\rho_{TaN} = 1\,e^{-5}$ Ohm m. It should be mentioned that such noticeable changes in the line resistance caused by void growth are generated only in the short lines with the length of 1 μm or less.

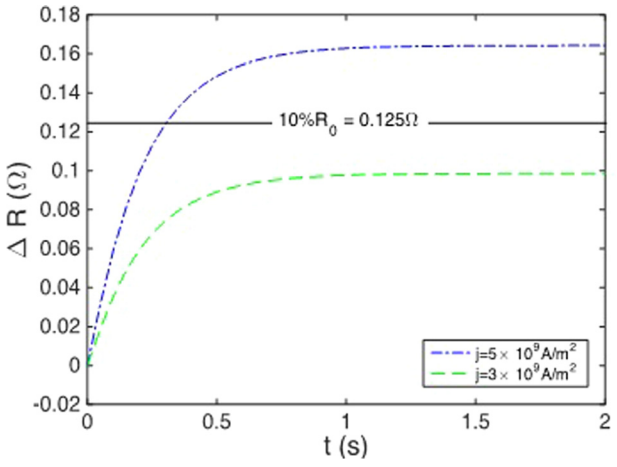

FIG. 8. $\Delta R(t)$ kinetics caused by the current densities of 3×10^9 A/m^2 and 5×10^9 A/m^2. Initial line resistance $R_0 = \rho_{Cu}L/WH = 1.25\ \Omega$, T = 400 K.

In the case of time-dependent current densities loaded to the line with the preexisted void, a calculation of the stress evolution is done in the way very similar to that was used for the calculation of stress evolution in the void-less case, considered in Section II. Conversion of the stress distribution obtained from the solution of Eq. (5), with the zero stress and zero flux BC at the void edge and the anode end of line correspondingly, to the void volume evolution, and, then, to the kinetics of the resistance change, similarly to how it was done for the DC load, provides the following results: for the general case of time-dependent current density $j(t)$: (global time is t)

$$\Delta R(t) = -\frac{4eZ\rho D_a}{\pi k_B T}\left(\frac{\rho_{TaN}}{h_{lin}(W+2H)} - \frac{\rho_{Cu}}{WH}\right) \times \sum_{k=1}^{\infty}\frac{(-1)^k}{(2k+1)}e^{-\kappa\frac{(2k+1)^2\pi^2}{4L^2}t}\int_0^t j(t)e^{\kappa\frac{(2k+1)^2\pi^2}{4L^2}\tau}d\tau \tag{15}$$

and for resistance relaxation after switching off the electric current at t_+: (global time is $t \geq t_+$)

$$\Delta R(t) = -\frac{4eZ\rho D_a}{\pi k_B T}\left(\frac{\rho_{TaN}}{h_{lin}(W+2H)} - \frac{\rho_{Cu}}{WH}\right) \times \sum_{k=1}^{\infty}\frac{(-1)^k}{(2k+1)}e^{-\kappa\frac{(2k+1)^2\pi^2}{4L^2}t}\int_0^{t_+} j(t)e^{\kappa\frac{(2k+1)^2\pi^2}{4L^2}\tau}d\tau. \tag{16}$$

Figure 9 shows the kinetics of line resistance change caused by a random time-dependent current, Fig. 9(a), and by switching off the applied current, Fig. 9(b).

Resistance evolutions resulted by the high frequency UPC and symmetrical and nonsymmetrical BPC loads are shown in Fig. 10. Analytical expressions describing these kinetics, which were obtained from the solution of Eq. (3) for different waveforms of the loaded current densities, are shown in Appendix B. It can be seen from Figs. 10(a) to 10(b) that the UPC load results the resistance increase, which is characterized by almost same rate as was obtained for the DC load, but by smaler value, proportional to the pulse duty factor. Due to a very short time interval between pulses any noticeable stress relaxation cannot occur. A symmetrical BPC causes an oscillation of the void volume and, hence, a resistance around their original values, Fig. 10(c). A quite different result of the symmetrical BPC load is observed, when the oscillating temperature is generated inside this metal line. Figure 10(d) shows the resistance increase caused by the symmetrical BPC, which is synchronized with a specific temperature oscillation: the positive pulse of the current happens at higher temperature than the negative pulse. It destroys the symmetry of the bidirectional change of the void volume caused by a transfer of atoms between the void

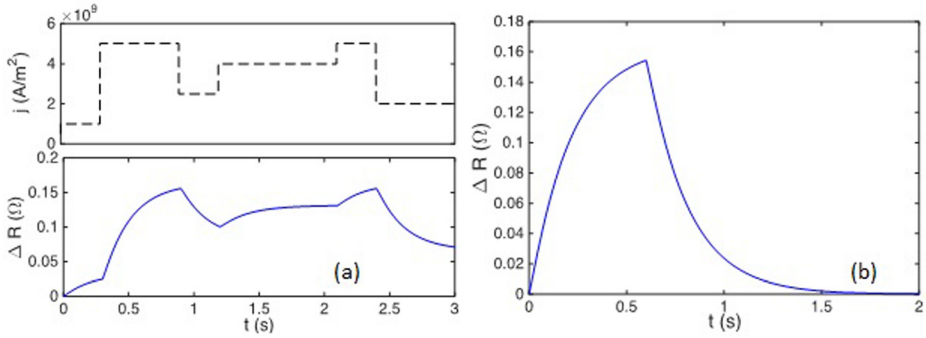

FIG. 9. Short line resistance evolution caused by a random set of current densities, (a); relaxation of the resistance change accumulated during 0.6 s of $j = 5 \times 10^9$ A/m^2 stressing, (b). $T = 400$ K for both cases.

surface and metal bulk. The resistance increase shown in Fig. 10(d) is happened when the current positive pulses forcing atoms to move from the void surface into the metal in the direction toward the anode end of line occur at $T = 450$ K, while the negative pulses pushing atoms back on the void surface take place at lower temperature of $T = 400$ K. We use this ideal but unrealistic synchronized current-temperature dynamics just to illustrate a possible mechanism of resistance degradation in short metal lines loaded with the symmetrical BPC. In reality, we can expect a variety of temperature oscillations inside on-chip interconnect due to a sporadic character of switching of many millions of transistors, which locations are distributed through the chip layout. Such irregular temperature oscillations can cause asymmetry in the void shrinking-advancing and, in some cases, can be responsible for void growth above the critical size, corresponding to the threshold increase of the line resistance.

IV. CONCLUSION

We have presented results of the analytic solution to continuity equation describing the stress evolution kinetics in the confined metal line with the diffusion blocking ends caused by a time-dependent electric current load. A number of cases characterized by different types of current wave forms were analyzed. A comparison of the predicted analytic stress evolution kinetics with the results generated by the direct numerical calculation of the continuity equation with the COMSOL FEA tool has demonstrated an excellent agreement.

A procedure for conversion of the time-dependent current load to the effective DC load based on the stress generation criteria was proposed. Analytic formulations of the effective DC currents in the general case of the time-dependent electric stressing and in particular, cases of unidirectional and bidirectional pulse currents were demonstrated.

It was demonstrated that EM caused by the symmetrical bidirectional electric stressing cannot be responsible for the stress-induced voiding due to small stress buildup. Different physical phenomena responsible for the failure should be identified. In addition to the discussed thermal fatigue, the paper proposes another possible mechanism of failure caused by symmetrical bidirectional currents. Very short metal lines with preexisted thermal voids, which are loaded with the bidirectional currents, can demonstrate a notable resistance increase when a specific temperature oscillation is generated in the line.

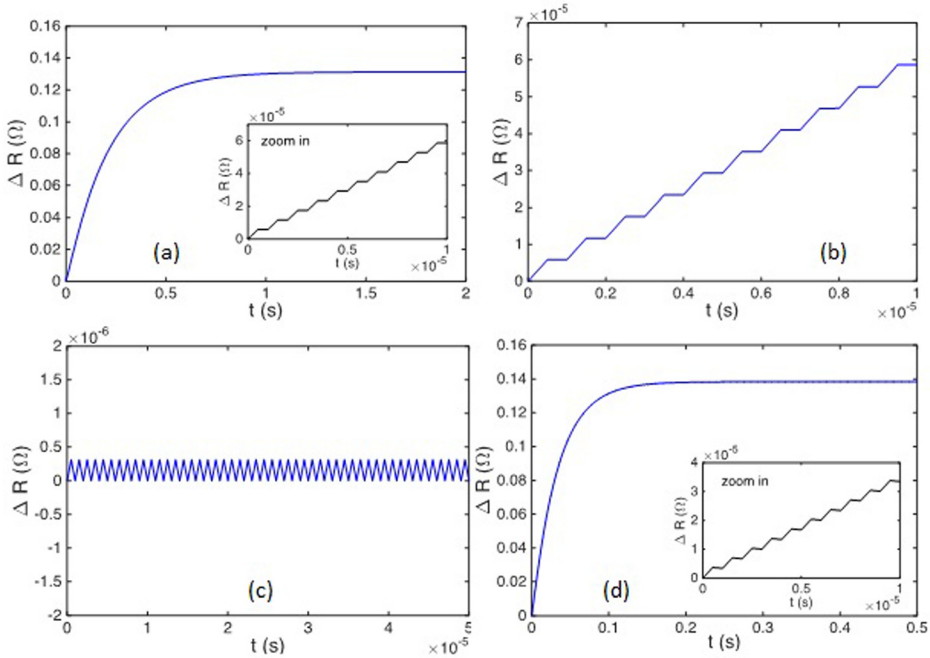

FIG. 10. 1 MHz UPC load with $j_+ = 8 \times 10^9$ A/m^2, $t^+ = T/2$, $T = 400$ K, (a); same UPC load at the smal time scale, (b); 1 MHz symmetrical BPC load with $j_+ = 5 \times 10^9$ A/m^2, $j_- = -5 \times 10^9$ A/m^2, $t^+ = t^- = T/2$, $T = 400$ K, (c); 1 MHz symmetrical BPC load with $j_+ = 5 \times 10^9$ A/m^2, $j_- = -5 \times 10^9$ A/m^2, $t^+ = t^- = T/2$, $T^+ = 450$ K, $T^- = 400$ K, (d).

ACKNOWLEDGMENTS

One of the authors (V. Sukharev) gratefully acknowledges inspirational discussions with Dr. R. Rosenberg of IBM T. J. Watson Research Center, Yorktown Heights, NY, and Dr. E. Zschech of Fraunhofer-IKTS, Dresden, Germany, and Dr. A. Kteyan of Mentor Graphics Corporation, Yerevan, Armenia. S. X.-D. Tan and X. Huang would like to thank National Science Foundation, NSF FRS (Failure Resistant Systems) program (Grant No. CCF-1255899), and Semiconductor Research Corporation, NSF/SRC Multi-core Program (Grant No. SRC 2013-TJ-2417) for the financial support of their research.

APPENDIX A: STRESS EVOLUTION CAUSED BY UPC AND BPC LOADS

Stress evolutions caused by a unipolar (unidirectional) pulse current with the density j_+, pulse period T, and pulse time t_+ can be obtained from solution of Eq. (5) with the initial condition: $\sigma(x,t=T)=\sigma_T+\frac{4eZ\rho}{\Omega l}\kappa\sum_{n=0}^{\infty}\cos\frac{(2n+1)\pi x}{l}e^{-\kappa\frac{(2n+1)^2\pi^2}{l^2}T}\int_0^{t_+}j_+(t)e^{\kappa\frac{(2n+1)^2\pi^2}{l^2}\tau}d\tau$. The kinetics has the form

$$\sigma(x,t)=\sigma_T+\frac{4eZ\rho}{\Omega l}\kappa\sum_{n=0}^{\infty}\cos\frac{(2n+1)\pi x}{l}e^{-\kappa\frac{(2n+1)^2\pi^2}{l^2}\tau}\times\left(\int_0^{\tau}j_+(\tilde{\tau})e^{\kappa\frac{(2n+1)^2\pi^2}{l^2}\tilde{\tau}}d\tilde{\tau}+e^{-\kappa\frac{(2n+1)^2\pi^2}{l^2}T}\int_0^{t_+}j_+(\tilde{\tau})e^{\kappa\frac{(2n+1)^2\pi^2}{l^2}\tilde{\tau}}d\tilde{\tau}\frac{1-e^{-\kappa\frac{(2n+1)^2\pi^2}{l^2}mT}}{1-e^{-\kappa\frac{(2n+1)^2\pi^2}{l^2}T}}\right). \tag{A1}$$

Here, $t=mT+\tau$ is the global time, Fig. 3.

Solution of Eq. (5) for the bipolar (bidirectional) pulse current with the positive and negative densities j_+ and j_-, pulse period T, and positive and negative phase durations t_+ and t_- results in the following stress evolution kinetics:

(1) For the positive pulse phase, global time is $t=mT+\tau$

$$\sigma(x,t)=\sigma_T+\frac{4eZ\rho}{\Omega l}\kappa\sum_{n=0}^{\infty}\cos\frac{(2n+1)\pi x}{l}e^{-\frac{\tau}{\tau_0^{(2n+1)}}}\times\left(\int_0^{\tau}j_+e^{\frac{\tilde{\tau}}{\tau_0^{(2n+1)}}}d\tilde{\tau}+\left(e^{-\frac{T}{\tau_0^{(2n+1)}}}\int_0^{t_+}j_+e^{\frac{\tilde{\tau}}{\tau_0^{(2n+1)}}}d\tilde{\tau}+e^{-\frac{t_-}{\tau_0^{(2n+1)}}}\int_0^{t_-}j_-e^{\frac{\tilde{\tau}}{\tau_0^{(2n+1)}}}d\tilde{\tau}\right)\frac{1-e^{-\frac{mT}{\tau_0^{(2n+1)}}}}{1-e^{-\frac{T}{\tau_0^{(2n+1)}}}}\right). \tag{A2}$$

(2) For the negative pulse phase, global time is

$$t=mT+t_++\tau, \tag{A3}$$

$$\sigma(x,t)=\sigma_T+\frac{4eZ\rho}{\Omega l}\kappa\sum_{n=0}^{\infty}\cos\frac{(2n+1)\pi x}{l}e^{-\frac{\tau}{\tau_0^{(2n+1)}}}\times\left(\int_0^{\tau}j_-e^{\frac{\tilde{\tau}}{\tau_0^{(2n+1)}}}d\tilde{\tau}+e^{-\frac{t_+}{\tau_0^{(2n+1)}}}\int_0^{t_+}j_+e^{\frac{\tilde{\tau}}{\tau_0^{(2n+1)}}}d\tilde{\tau}+e^{-\frac{T}{\tau_0^{(2n+1)}}}\left(e^{-\frac{t_+}{\tau_0^{(2n+1)}}}\int_0^{t_+}j_+e^{\frac{\tilde{\tau}}{\tau_0^{(2n+1)}}}d\tilde{\tau}+\int_0^{t_-}j_-e^{\frac{\tilde{\tau}}{\tau_0^{(2n+1)}}}d\tilde{\tau}\right)\frac{1-e^{-\frac{mT}{\tau_0^{(2n+1)}}}}{1-e^{-\frac{T}{\tau_0^{(2n+1)}}}}\right). \tag{A4}$$

APPENDIX B: STRESS AND RESISTANCE EVOLUTIONS CAUSED BY UPC AND BPC LOADS IN A LINE WITH THE PREEXISTED VOID

Stress evolutions caused by a UPC with the density j_+, pulse period T, and pulse time t_+ can be obtained from solution of Eq. (5) with the initial condition: $\sigma(x,t=T)=0$, and the zero stress and zero flux BC at the void edge and the anode end of line correspondingly. The kinetics has the form

$$\sigma(x,t)=-\frac{2eZ\rho}{\Omega L}\kappa\sum_{k=1}^{\infty}(-1)^k\sin\frac{(2k+1)\pi x}{2L}e^{-\kappa\frac{(2k+1)^2\pi^2}{4L^2}\tau}\times\left(\int_0^{\tau}j_+(\tilde{\tau})e^{\kappa\frac{(2k+1)^2\pi^2}{4L^2}\tilde{\tau}}d\tilde{\tau}+e^{-\kappa\frac{(2k+1)^2\pi^2}{4L^2}T}\int_0^{t_+}j_+(\tilde{\tau})e^{\kappa\frac{(2k+1)^2\pi^2}{4L^2}\tilde{\tau}}d\tilde{\tau}\frac{1-e^{-\kappa\frac{(2k+1)^2\pi^2}{4L^2}mT}}{1-e^{-\kappa\frac{(2k+1)^2\pi^2}{4L^2}T}}\right). \tag{B1}$$

Here, $t=mT+\tau$ is the global time, Fig. 3. Corresponding resistance evolution has the form

$$\Delta R(t)=-\frac{4eZ\rho D_a}{\pi k_BT}\left(\frac{\rho_{TaN}}{h_{lin}(W+2H)}-\frac{\rho_{Cu}}{WH}\right)\sum_{k=1}^{\infty}\frac{(-1)^k}{(2k+1)}e^{-\kappa\frac{(2k+1)^2\pi^2}{4L^2}\tau}\times\left(\int_0^{\tau}j_+(\tilde{\tau})e^{\kappa\frac{(2k+1)^2\pi^2}{4L^2}\tilde{\tau}}d\tilde{\tau}+e^{-\kappa\frac{(2k+1)^2\pi^2}{4L^2}T}\int_0^{t_+}j_+(\tilde{\tau})e^{\kappa\frac{(2k+1)^2\pi^2}{4L^2}\tilde{\tau}}d\tilde{\tau}\frac{1-e^{-\kappa\frac{(2k+1)^2\pi^2}{4L^2}mT}}{1-e^{-\kappa\frac{(2k+1)^2\pi^2}{4L^2}T}}\right). \tag{B2}$$

Solution of Eq. (5) for the BPC with the positive and negative densities j_+ and j_-, pulse period T, and positive and negative phase durations t_+ and t_- results in the following stress evolution kinetics:

For the positive pulse phase, global time is $t = mT + \tau$

$$\sigma(x,t) = -\frac{2eZ\rho}{\Omega L}\kappa\sum_{k=1}^{\infty}(-1)^k \sin\frac{(2k+1)\pi x}{2L} e^{-\frac{\tau}{\tau_{0,2k+1}}} \times \left(\int_0^{\tau} j_+ e^{\frac{\tilde{\tau}}{\tau_{0,2k+1}}} d\tilde{\tau} + \left(e^{-\frac{T}{\tau_{0,2k+1}}}\int_0^{t_+} j_+ e^{\frac{\tilde{\tau}}{\tau_{0,2k+1}}} d\tilde{\tau} + e^{-\frac{t_-}{\tau_{0,2k+1}}}\int_0^{t_-} j_- e^{\frac{\tilde{\tau}}{\tau_{0,2k+1}}} d\tilde{\tau}\right)\frac{1-e^{-\frac{mT}{\tau_{0,2k+1}}}}{1-e^{-\frac{T}{\tau_{0,2k+1}}}}\right). \quad \text{(B3)}$$

And the resistance evolution is

$$\Delta R(t) = -\frac{4eZ\rho D_a}{\pi k_B T}\left(\frac{\rho_{TaN}}{h_{lin}(W+2H)} - \frac{\rho_{Cu}}{WH}\right)\sum_{k=1}^{\infty}\frac{(-1)^k}{(2k+1)} e^{-\frac{\tau}{\tau_{0,2k+1}}} \times \left(\int_0^{\tau} j_+ e^{\frac{\tilde{\tau}}{\tau_{0,2k+1}}} d\tilde{\tau} + \left(e^{-\frac{T}{\tau_{0,2k+1}}}\int_0^{t_+} j_+ e^{\frac{\tilde{\tau}}{\tau_{0,2k+1}}} d\tilde{\tau} + e^{-\frac{t_-}{\tau_{0,2k+1}}}\int_0^{t_-} j_- e^{\frac{\tilde{\tau}}{\tau_{0,2n+1}}} d\tilde{\tau}\right)\frac{1-e^{-\frac{mT}{\tau_{0,2k+1}}}}{1-e^{-\frac{T}{\tau_{0,2k+1}}}}\right). \quad \text{(B4)}$$

For the negative pulse phase, global time is $t = mT + t_+ + \tau$, the stress evolution kinetics is

$$\sigma(x,t) = -\frac{2eZ\rho}{\Omega L}\kappa\sum_{k=1}^{\infty}(-1)^k \sin\frac{(2k+1)\pi x}{2L} e^{-\frac{\tau}{\tau_{0,2k+1}}} \times \left(\int_0^{\tau} j_- e^{\frac{\tilde{\tau}}{\tau_{0,2k+1}}} d\tilde{\tau} + e^{-\frac{t_+}{\tau_{0,2k+1}}}\int_0^{t_+} j_+ e^{\frac{\tilde{\tau}}{\tau_{0,2k+1}}} d\tilde{\tau} + e^{-\frac{T}{\tau_{0,2k+1}}}\left(e^{-\frac{t_+}{\tau_{0,2k+1}}}\int_0^{t_+} j_+ e^{\frac{\tilde{\tau}}{\tau_{0,2k+1}}} d\tilde{\tau} + \int_0^{t_-} j_- e^{\frac{\tilde{\tau}}{\tau_{0,2k+1}}} d\tilde{\tau}\right)\frac{1-e^{-\frac{mT}{\tau_{0,2k+1}}}}{1-e^{-\frac{T}{\tau_{0,2k+1}}}}\right). \quad \text{(B5)}$$

And the resistance evolution is

$$\Delta R(t) = -\frac{4eZ\rho D_a}{\pi k_B T}\left(\frac{\rho_{TaN}}{h_{lin}(W+2H)} - \frac{\rho_{Cu}}{WH}\right)\sum_{k=1}^{\infty}\frac{(-1)^k}{(2k+1)} e^{-\frac{\tau}{\tau_{0,2k+1}}} \times \left(\int_0^{\tau} j_- e^{\frac{\tilde{\tau}}{\tau_{0,2k+1}}} d\tilde{\tau} + e^{-\frac{t_+}{\tau_{0,2k+1}}}\int_0^{t_+} j_+ e^{\frac{\tilde{\tau}}{\tau_{0,2k+1}}} d\tilde{\tau} + e^{-\frac{T}{\tau_{0,2k+1}}}\left(e^{-\frac{t_+}{\tau_{0,2k+1}}}\int_0^{t_+} j_+ e^{\frac{\tilde{\tau}}{\tau_{0,2k+1}}} d\tilde{\tau} + \int_0^{t_-} j_- e^{\frac{\tilde{\tau}}{\tau_{0,2k+1}}} d\tilde{\tau}\right)\frac{1-e^{-\frac{mT}{\tau_{0,2k+1}}}}{1-e^{-\frac{T}{\tau_{0,2k+1}}}}\right). \quad \text{(B6)}$$

As before: $\tau_{0,2k+1} = \frac{4L^2}{\kappa\pi^2(2k+1)^2}$.

[1]X. Huang, T. Yu, V. Sukharev, and S. X.-D. Tan, "Physics-based electromigration assessment for power grid networks," in *Proceedings of the 51st Annual Design Automation Conference (DAC), San Francisco, CA, 1–5 June 2014*, pp. 1–6.

[2]J. A. Maiz, "Characterization of electromigration under bidirectional (BC) and pulsed unidirectional (PDC) currents," in *Proceedings of the 27th International Reliability Physics Symposium, 11–13 April 1989*, pp. 220–228.

[3]B. K. Liew, N. W. Cheung, and C. Hu, IEEE Trans. Electron Devices **37**, 1343 (1990).

[4]K. Hatanaka, T. Noguchi, and K. Maeguchi, "A threshold pulse width for electromigration under pulsed stress conditions," in *Proceedings of the Sixth International IEEE VLSI Multilevel Interconnection Conference, Santa Clara, CA, 12–13 June 1989*, pp. 183–189.

[5]H. Chenming, Microelectron. Reliab. **38**, 1 (1998).

[6]W. R. Hunter, IEEE Trans. Electron Devices **44**, 304 (1997); **44**, 310 (1997).

[7]M. A. Korhonen, P. Borgesen, K. N. Tu, and C. Y. Li, J. Appl. Phys. **73**, 3790 (1993).

[8]Z. Suo, in *Reliability of Interconnect Structures*, Interfacial and Nanoscale Failure Vol. 8, edited by W. Gerberich and W. Yang, Comprehensive Structural Integrity (Elsevier, Amsterdam, 2003), pp. 265–324.

[9]I. A. Blech and C. Herring, Appl. Phys. Lett. **29**, 131 (1976).

[10]F. F. Abraham, *Homogeneous Nucleation Theory* (Academic Press, New York, 1974).

[11]COMSOL, Inc., Burlington, MA. 8 New England Executive Park.

[12]P. Jain, S. S. Sapatnekar, and J. Cortadella, "A retargetable and accurate methodology for logic-IP-internal electromigration assessment," in *Proceedings of the ASP-DAC, Chiba, Japan, 19–22 January 2015*, pp. 346–351.

[13]R. Moning, R. R. Keller, and C. A. Volkert, Rev. Sci. Instrum. **75**, 4997 (2004).

[14]J. Tao, N. W. Cheung, and C. Hu, IEEE Electron Device Lett. **14**, 554 (1993).

[15]L. M. Ting, J. S. May, W. R. Hunter, and J. W. McPherson, "AC electromigration characterization and modeling of multilayered interconnects," in *Proceedings of the 31st International Reliability Physics Symposium, 23–15 March 1993*, pp. 311–316.

[16]K.-D. Lee, "Electromigration recovery and short lead effect under bipolar- and unipolar-pulse current," in *Proceedings of the International Reliability Physics Symposium, 15–19 April 2012*, pp. 6B.3.1–6B.3.4.
[17]M. A. Meyer, M. Herrmann, E. Langer, and E. Zschech, Microelectron. Eng. **64**, 375 (2002).
[18]J. He and Z. Suo, "Statistics of electromigration lifetime analyzed using a deterministic transient model," AIP Conf. Proc. **741**, 15–26 (2004).
[19]J. He, Z. Suo, T. N. Marieb, and J. A. Maiz, Appl. Phys. Lett. **85**, 4639 (2004).